Application and Validation of External Condensation Models for Horizontal Tubes in MARS-KS

Taeyeon Min, Yeongjae Cho, Jeong Ik Lee *
Department of Nuclear and Quantum Engineering, N7-1 KAIST, 291 Daehak-ro, Yuseong-gu, Daejeon, Korea 34141
**Corresponding author: jeongiklee@kaist.ac.kr*

***Keywords:** Small Modular Reactor, MARS-KS, Condensation, Horizontal Tube, Vapor Shear*

1. Introduction

The innovative Small Modular Reactor (i-SMR) under development in Korea adopts an integral pressurized water reactor (iPWR) configuration in which the core, pressurizer, reactor coolant pumps, and helical-coil steam generator (SG) are integrated within the reactor vessel. In addition, a dry metal containment vessel is maintained under vacuum during normal operation [1]. During a rupture of the Modular Makeup and Purification System (MMPS) charging line, the reactor-vessel pressure and water level decrease, allowing steam to occupy the outer annular region surrounding the SG. After passive cooling is established, heat removal through the SG tubes induces condensation on their external surfaces, and the condensate drains toward the core region. Figure 1 illustrates the resulting CV-RV recirculation path.

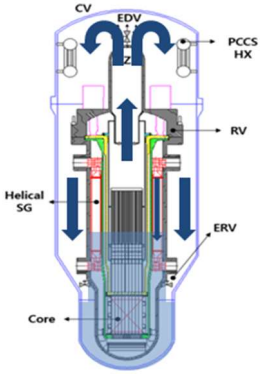


Fig 1. Condensation and CV-RV recirculation scheme in the i-SMR under accident conditions.

Reliable prediction of external condensation is required for system-level safety analysis. The condensation models currently available in thermal-hydraulic system codes were not originally developed for this geometry. In MARS-KS, the wall-condensation treatment employs classical correlations such as the Nusselt, Shah, and Chato models, which represent laminar film condensation on a simple surface or condensation inside a tube [2,3,4]. External condensation on a horizontal tube in cross-flow is physically different because the condensate film drains around the tube circumference while the incoming vapor exerts interfacial shear on the film. For a tube bank, condensate formed on an upper tube may also fall onto lower tubes, increasing the local film flow rate and reducing the heat-transfer coefficient. Thus, vapor shear, condensate inundation, and the external-tube geometry should all be considered when assessing the applicability of a system-code condensation model to the i-SMR SG.

A direct model for the complete helical geometry is ultimately required; however, a horizontal-tube model provides a useful first validation step. The i-SMR SG has a relatively small tube-to-coil diameter ratio, indicating a relatively weak curvature effect. Karimi showed that, as the curvature effect decreases, the condensation heat transfer coefficient (HTC) of a helical tube approaches that of an inclined circular tube [5]. For the i-SMR geometric range considered in the present work, the helical correction factor is expected to be close to unity, whereas uncertainties associated with film drainage, vapor shear, inundation, and system-code geometric interpretation remain significant. Figure 2 illustrates the principal effects of vapor shear and condensate inundation on the condensate film. Therefore, the present study first isolates these uncertainties using horizontal-tube condensation data before extending the model to a high-pressure helical-tube configuration.

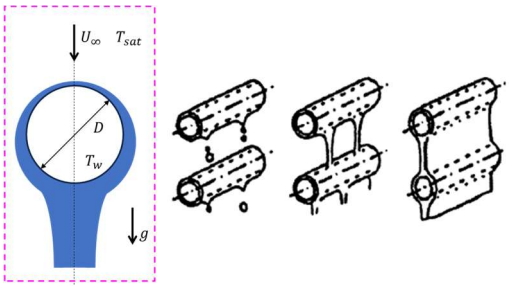


Fig 2. Schematic of vapor shear and condensate inundation effects on film condensation.

The objective of this study is to apply and validate an external horizontal-tube condensation model in MARS-KS. First, the geometric treatment of the default Nusselt-type film model is examined and modified so that the characteristic film flow is determined from the physical heated perimeter rather than a user-specified heated equivalent diameter. Second, the forced-convection correction proposed by Rose is applied to represent the enhancement caused by vapor shear [6]. The geometry-corrected cross-flow model and the shear-corrected model are then compared with 405 experimental data points obtained from three independent steam-

condensation studies covering single-tube, tube-bank, and artificial-inundation conditions [7–9]. The purpose is not to claim direct validation under the target i-SMR accident conditions, but to establish a physically consistent baseline model and to identify the remaining uncertainties that must be resolved by dedicated high-pressure experiments.

In the present work, the geometric correction is limited to the local film-flow representation of an individual horizontal tube. Condensate inundation between successive tube rows is not introduced as a separate closure model; instead, the inundation ratio is used to characterize the experimental database and to assess the remaining model uncertainty.

2. Methodology

The MARS-KS v2.0 condensation subroutine was reviewed with emphasis on the liquid-film contribution to the wall heat-transfer coefficient. In the default formulation used for the present cases, the condensation coefficient is obtained from the condensate thermal conductivity divided by an estimated film thickness, following a Nusselt-type treatment. The film thickness is obtained from a film Reynolds number, and the Reynolds number uses the heated equivalent diameter.

$$h_c = \frac{k_f}{\delta} \tag{1}$$

$$\delta = \left[\frac{3\mu_f^2 Re_{film}}{4g\rho_f\Delta\rho}\right]^{\frac{1}{3}} \tag{2}$$

$$Re_{film} = \frac{G_f D_{heat}}{\mu_f} \tag{3}$$

This treatment creates an inconsistency when external condensation and cross-flow convection are evaluated for the same tube geometry. In the MARS-KS helical SG convection model, the Zukauskas correlation uses the tube diameter as the characteristic length. In contrast, the default condensation treatment requires a heated equivalent diameter based on $4A/P_{heat}$. Consequently, a user-specified heated diameter cannot consistently represent both heat-transfer modes.

2.1 Cross-Flow Geometry-Corrected Model and Conceptual Verification

To resolve this inconsistency, a dedicated heat-structure boundary option was introduced for external-tube cross-flow condensation while leaving the existing MARS-KS treatment for other heat structures unchanged. In the modified model, the condensate film mass flux is evaluated directly from the local liquid mass flow rate as

$$\delta = \left[\frac{3\mu_f^2 \Gamma_f}{g\rho_f\Delta\rho}\right]^{\frac{1}{3}} \tag{4}$$

$$\Gamma_f = \frac{\dot{m}_f}{P_{he}} \tag{5}$$

where $\dot{m}_f$is the condensate mass flow rate and P_{heat} is the effective film-flow perimeter. For a horizontal tube, condensate drains along both sides of the tube, and P_{heat} is therefore taken as twice the tube length, $2L$. In the code, this value is calculated directly from the heat-transfer area and tube radius. The liquid-film thickness is then evaluated from the existing Nusselt-type film relation using Γ_f and the condensation HTC is calculated using Eq. (3), as in the default model. Thus, the modified condensation calculation no longer depends on the user-specified heated equivalent diameter.

A conceptual verification was performed to confirm that the modified calculation reproduces the intended condensation behavior while removing the dependence on the heated-diameter input. Three cases were considered. Case 1 used the default MARS-KS model with the heated equivalent diameter defined as $4A/P_{heat}$, representing the appropriate geometric treatment for condensation. Case 2 used the default model with D_{tube} as the heated diameter, corresponding to the diameter required by the Zukauskas model. Case 3 used the cross-flow geometry-corrected model implemented in MARS-KS. The modified model is considered conceptually consistent if Case 3 reproduces the condensation behavior of Case 1 while allowing the tube diameter required for the convection model to be used as the common geometric input.

The reference geometry consists of a single horizontal tube located in a rectangular duct. The shell-side duct has a width and length of 0.5 m and a height of 1.0 m, while the tube has an outer diameter of 15 mm and a heated length of 0.5 m. Saturated steam flows downward through the shell side at a mass flow rate of 0.1 kg/s and a pressure of 1 atm, with an inlet quality of 1.0. The tube wall is maintained at a constant temperature corresponding to a wall subcooling of 10 K. Tables I and II summarize the geometry and thermal-hydraulic boundary conditions used for the conceptual verification.

Table I. Geometry for conceptual verification

Shell side	Width	0.5 m
	Length	0.5 m
	Height	1.0 m
Tube side	Diameter	15 mm
	Length	0.5 m

Table II. Boundary conditions for conceptual verification

Shell side	Mass flow rate	0.1 kg/s
	Pressure	1 atm
	Quality	1.0
Tube wall	Wall subcooling	10 K

Figure 3 shows the MARS-KS nodalization used for the calculation. The shell side was represented by a pipe component consisting of 10 control volumes, and the horizontal condensation tube was located in the fifth control volume. A constant-temperature heat structure

was connected to this control volume to simulate external steam condensation. Because the three cases employ identical nodalization and thermal-hydraulic boundary conditions, differences in the predicted condensation heat-transfer coefficient can be attributed directly to the treatment of the heated equivalent diameter and condensate film flow. The present correction addresses only the local film-flow geometry of each tube and does not explicitly model inter-row condensate transfer or redistribution within a tube bank.

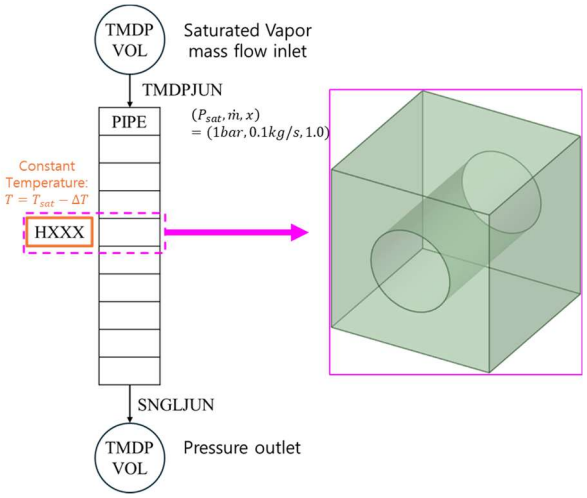


Fig 3. Input modeling for conceptual verification.

2.2 Vapor-Shear-Corrected Model and Validation

Vapor shear was incorporated using the Rose condensation correlation. This model introduces a dimensionless shear parameter F and a two-phase Reynolds number, Re_{tp}.

$$Nu_{Rose}Re_{tp}^{\frac{1}{2}} = \frac{0.9 + 0.728F^{\frac{1}{2}}}{\left(1 + 3.44F^{\frac{1}{2}} + F\right)^{\frac{1}{4}}} \quad (6)$$

$$F = \frac{\mu_{film} h_{fg} g D}{k_{film} U_{\infty}^2 \Delta T} \quad (7)$$

$$Re_{tp} = \frac{\rho_{film} U_{\infty} D}{\mu_{film}} \quad (8)$$

where U_∞ is the free-stream vapor velocity. The parameter F represents the relative importance of gravity and vapor shear in determining the motion of the condensate film. A smaller F corresponds to a stronger vapor-shear effect. As the vapor velocity approaches zero (F→∞), Eq. (6) asymptotically approaches the Nusselt model given by Eq. (9)

$$Nu = 0.728F^{1/4}Re_{tp}^{\frac{1}{2}} = 0.728\left(\frac{\rho_l^2 g h_{fg} D^3}{\mu_l k_l \Delta T}\right)^{\frac{1}{4}} \quad (9)$$

In the code implementation, the Rose-to-Nusselt ratio is calculated as a multiplicative correction factor and applied to the condensation coefficient obtained from the geometry-corrected film model. In the original correlation, U_∞ represents the free-stream vapor velocity. In the MARS-KS implementation, U_∞ is approximated using the upstream junction gas velocity, $U_{g,up,junc}$, which represents the vapor approaching the control volume connected to the heat structure. The flow diagram is shown in Figure 4. This treatment was activated only for the newly defined external-tube boundary option.

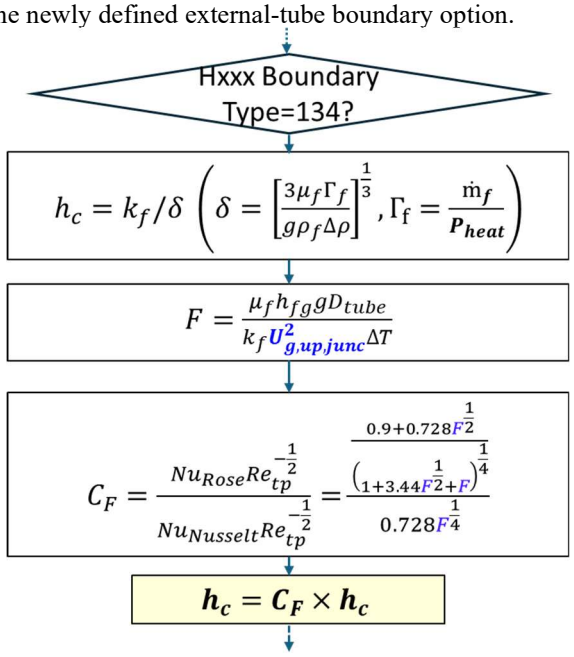


Fig 4. Implementation of the vapor-shear correction in MARS-KS.

Three experimental databases were used for model validation. Murase et al. provided 10 single-tube data points with controlled condensate inundation [7]. Nobbs reported 345 data points for downward steam flow over horizontal tubes and tube banks with square and triangular arrangements, covering variations in vapor velocity, inundation, coolant temperature, and bundle geometry [8]. Demirel provided 50 data points from five vertically arranged tubes under 10 cooling-water flow-rate conditions [9]. In total, 405 condensation heat-transfer coefficients were used for model evaluation.

The database was organized using two parameters that directly characterize the physical mechanisms represented by the model: the Rose shear parameter F and the inundation ratio defined as the incoming condensate flow from above divided by the condensate generated on the evaluated tube. Figures 5 and 6 show the experimental condensation HTCs as functions of the Rose shear parameter F and the inundation ratio, respectively.

Prediction performance was quantified using the mean absolute percentage error, defined as follows:

$$MAPE = \frac{100}{n}\sum_{i=1}^{n}\left|\frac{A_i - P_i}{A_i}\right| \quad (10)$$

where A_i and P_i are the measured and predicted heat-transfer coefficients. In addition, the fractions of overpredicted and underpredicted data were evaluated because models with similar MAPE can exhibit

substantially different conservative or non-conservative biases. The two model variants were compared using identical experimental inputs so that differences would originated only from the condensation treatment. For each experimental case, the MARS-KS input was constructed using a nodalization similar to that employed in the conceptual verification, except that the heat structure was coupled to an explicit cooling-water loop rather than prescribed with a constant wall temperature. The cooling-water inlet temperature and mass flow rate, together with the steam-side saturation pressure and mass flow rate, were specified according to the corresponding experimental conditions.

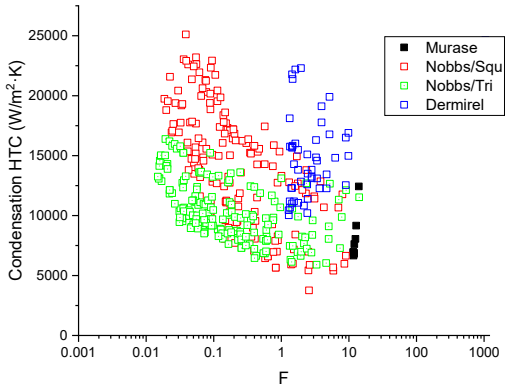


Fig 5. Experimental condensation HTC as a function of the Rose shear parameter *F*.

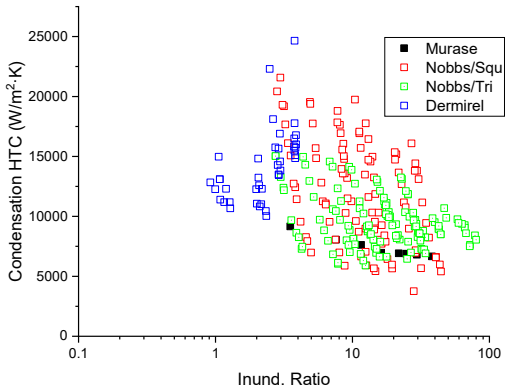


Fig 6. Experimental condensation HTC as a function of the inundation ratio.

3. Results

3.1 Conceptual Verification

Figure 7 presents the conceptual verification results. The default model using D_{tube} substantially overpredicted the condensation HTC, whereas the modified MARS-KS model predicted a value close to both the theoretical value of 14,311 W/m²·K given by Eq. (9) and the value predicted by the default model using $4A/P_{heat}$. This confirms that the modified formulation removes the dependence of the condensation calculation on the user-specified heated diameter while preserving the intended film-condensation behavior.

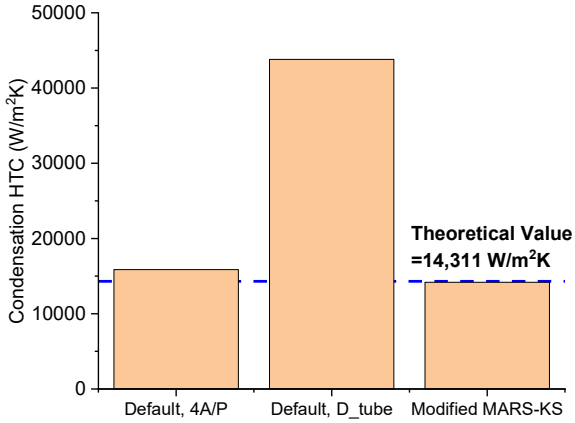


Fig 7. Results of Conceptual verification.

3.2 Validation using the Experimental Database

As shown in Figures 5 and 6, the condensation heat-transfer coefficient generally increases as F decreases and decreases as the inundation ratio increases. These trends are consistent with the enhancement caused by vapor shear and the increased film resistance caused by additional condensate loading.

Figures 8 and 9 compare the measured condensation HTCs with the predictions of the cross-flow geometry-corrected and Rose shear-corrected models, respectively. The cross-flow geometry correction removed the artificial dependence of the film-thickness calculation on the user-specified heated equivalent diameter, although the overall MAPE was 51.2%. When the Rose shear correction was subsequently applied, the overall MAPE decreased to 32.6%, providing the best agreement among the evaluated models. However, 31.4% of the data were overpredicted, particularly in the low-*F* region where vapor shear is strongest. This suggests that an additional limiter or transition treatment may be required for strong-shear conditions. The present model does not include a dedicated closure for condensate inundation. Therefore, although the inundation ratio is useful for identifying the reduction in HTC associated with additional condensate loading, detailed phenomena such as condensate impingement, redistribution, and row-to-row drainage are not explicitly resolved and may contribute to the remaining prediction error.

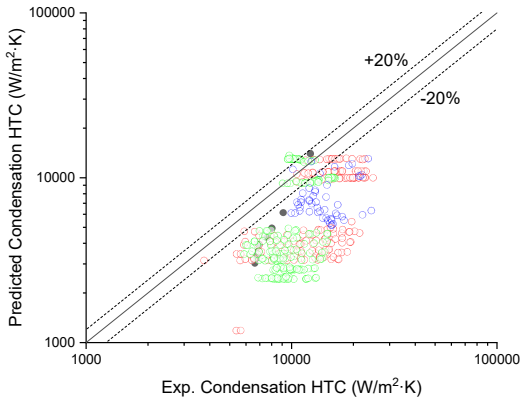


Fig 8. Experimental versus predicted condensation HTC for the cross-flow geometry-corrected model.

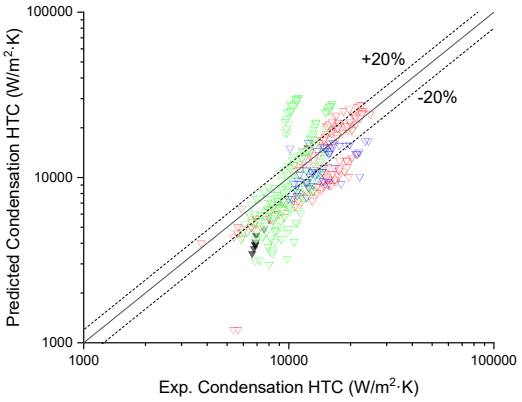


Fig 9. Experimental versus predicted condensation HTC for the Rose shear-corrected model.

4. Conclusions

This study modified the MARS-KS condensation model for external horizontal-tube condensation as a preliminary step toward application to the i-SMR helical SG. The cross-flow formulation removed the dependence of the film-thickness calculation on the user-specified heated equivalent diameter, and conceptual verification confirmed that the modified model reproduced the intended Nusselt-type condensation behavior.

The model was further extended by applying the Rose vapor-shear correction and evaluated against 405 steam-condensation data points. The Rose-corrected model reduced the overall MAPE to 32.6%, providing the best agreement among the evaluated models. However, overprediction remained in the strong-shear region, indicating that additional refinement of the shear correction is required.

The available experimental database does not fully cover the high-pressure and high-inundation conditions relevant to the i-SMR MMPS charging-line-break scenario. Further validation under these conditions will therefore be conducted before extending the present horizontal-tube model to the actual helical SG geometry.

ACKNOWLEDGEMENTS

This work was supported by the Innovative Small Modular Reactor Development Agency grant funded by the Korea Government (MCEE) (No. RS-202400404240).

REFERENCES

[1] S. G. Lim, H. S. Nam, D. H. Lee, and S. W. Lee, "Design characteristics of nuclear steam supply system and passive safety system for Innovative Small Modular Reactor (i-SMR)," Nuclear Engineering and Technology, vol. 57, no. 10, 2025.
[2] W. Nusselt, "Die Oberflächenkondensation des Wasserdampfes," Zeitschrift des Vereines Deutscher Ingenieure, vol. 60, pp. 541-546 and 569-575, 1916.
[3] M. M. Shah, "A general correlation for heat transfer during film condensation inside pipes," International Journal of Heat and Mass Transfer, vol. 22, no. 4, pp. 547-556, 1979.
[4] J. C. Chato, "Laminar condensation inside horizontal and inclined tubes," ASHRAE Journal, vol. 4, pp. 52-60, 1962.
[5] A. Karimi, "Laminar film condensation on helical reflux condensers and related configurations," International Journal of Heat and Mass Transfer, vol. 20, pp. 1137-1144, 1977.
[6] J. W. Rose, "Approximate equations for forced convection condensation in the presence of a non-condensing gas on a flat plate and horizontal tube," International Journal of Heat and Mass Transfer, vol. 23, pp. 539-546, 1980.
[7] T. Murase, H. S. Wang, and J. W. Rose, "Effect of inundation for condensation of steam on smooth and enhanced condenser tubes," International Journal of Heat and Mass Transfer, vol. 49, pp. 3180-3189, 2006.
[8] D. W. Nobbs, "The effect of downward vapour velocity and inundation on the condensation rates on horizontal tubes and tube banks," Ph.D. Thesis, University of Bristol, 1975.
[9] I. Demirel, "The effect of condensate inundation on condensation heat transfer in tube bundles of marine condensers," M.S. Thesis, Naval Postgraduate School, 1980.